ACS Biomaterials SCIENCE & ENGINEERING
Article
Cite This: ACS Biomater. Sci. Eng. 2018, 4, 1558−1567

Electroconductive Gelatin Methacryloyl-PEDOT:PSS Composite Hydrogels: Design, Synthesis, and Properties

Andrew R. Spencer,[†] Asel Primbetova,[†] Abigail N. Koppes,[†,‡] Ryan A. Koppes,[†] Hicham Fenniri,[*,†,§,∥] and Nasim Annabi[*,†,⊥,#]

[†]Department of Chemical Engineering, [‡]Department of Biology, [§]Department of Chemistry and Chemical Biology, and [∥]Department of Bioengineering, Northeastern University, 360 Huntington Avenue, Boston, Massachusetts 02115-5000, United States

[⊥]Biomaterials Innovation Research Center, Brigham and Women's Hospital, Harvard Medical School, 65 Landsdowne Street, Boston, Massachusetts 02139, United States

[#]Harvard-MIT Division of Health Sciences and Technology, Massachusetts Institute of Technology, 77 Massachusetts Avenue, Cambridge, Massachusetts 02139, United States

Supporting Information

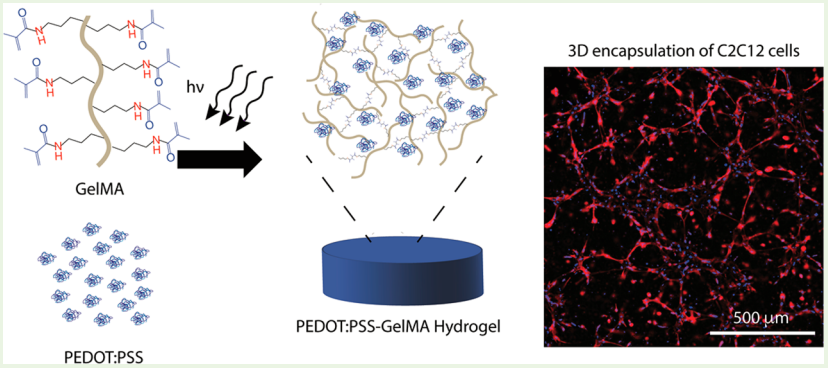

ABSTRACT: Electroconductive hydrogels are used in a wide range of biomedical applications, including electrodes for patient monitoring and electrotherapy, or as biosensors and electrochemical actuators. Approaches to design electroconductive hydrogels are often met with low biocompatibility and biodegradability, limiting their potential applications as biomaterials. In this study, composite hydrogels were prepared from a conducting polymer complex, poly(3,4-ethylenedioxythiophene):polystyrenesulfonate (PEDOT:PSS) dispersed within a photo-crosslinkable naturally derived hydrogel, gelatin methacryloyl (GelMA). To determine the impact of PEDOT:PSS loading on physical and microstructural properties and cellular responses, the electrical and mechanical properties, electrical properties, and biocompatibility of hydrogels loaded with 0−0.3% (w/v) PEDOT:PSS were evaluated and compared to GelMA control. Our results indicated that the properties of the hydrogels, such as mechanics, degradation, and swelling, could be tuned by changing the concentration of PEDOT:PSS. In particular, the impedance of hydrogels decreased from 449.0 kOhm for control GelMA to 281.2 and 261.0 kOhm for hydrogels containing 0.1% (w/v) and 0.3% (w/v) PEDOT:PSS at 1 Hz frequency, respectively. In addition, an *ex vivo* experiment demonstrated that the threshold voltage to stimulate contraction in explanted abdominal tissue connected by the composite hydrogels decreased from 9.3 ± 1.2 V for GelMA to 6.7 ± 1.5 V and 4.0 ± 1.0 V for hydrogels containing 0.1% (w/v) and 0.3% (w/v) PEDOT:PSS, respectively. *In vitro* studies showed that composite hydrogels containing 0.1% (w/v) PEDOT:PSS supported the viability and spreading of C2C12 myoblasts, comparable to GelMA controls. These results indicate the potential of our composite hydrogel as an electroconductive biomaterial.

KEYWORDS: *electroconductive, hydrogel, composite, conductive polymer, PEDOT:PSS, gelatin*

1. INTRODUCTION

Electroconductive hydrogels have shown promise in a wide range of applications where a mechanically flexible and hydrated conductive material is required, such as coatings on electrodes for monitoring and/or defibrillation,[1−3] implantable neural electrodes,[4−6] on-demand drug delivery vehicles,[7] soft actuators,[8] and tactile sensors.[9] Devices and materials that are intended to interface with tissues should be engineered to closely match both the physical and chemical properties of the target tissue. Because the function of both neural and muscle tissue is highly dependent on electrochemical signaling between or within cells,[10] materials that interact with them should also

Received: February 4, 2018
Accepted: March 5, 2018
Published: March 5, 2018

DOI: 10.1021/acsbiomaterials.8b00135
ACS Biomater. Sci. Eng. 2018, 4, 1558−1567

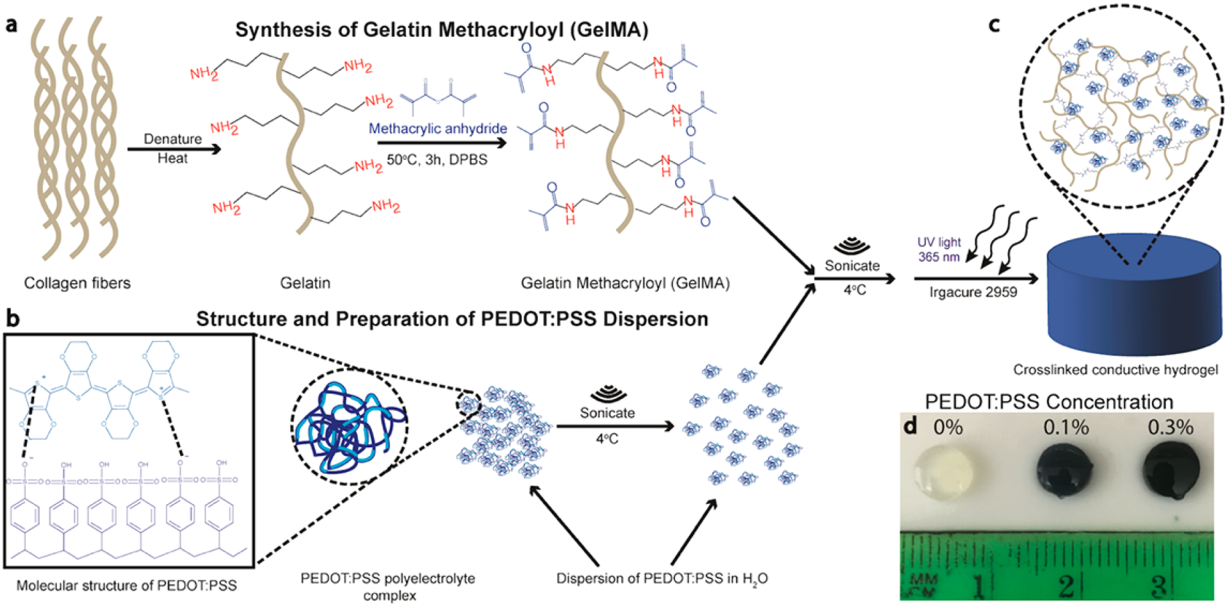

Figure 1. Preparation of GelMA/PEDOT:PSS hydrogels. (a) Schematic of GelMA preparation. (b) Preparation of PEDOT:PSS before mixing with GelMA precursor solution. (c) Photopolymerization of the precursor solutions to produce crosslinked hydrogel network. (d) Representative images of crosslinked hydrogels at varying concentration of PEDOT:PSS, including 0, 0.1, and 0.3%.

be designed with electroconductivity similar to the native tissue. Cardiac muscle and neural tissues often exhibit low regenerative potential, which has inspired the development of electroconductive and biocompatible materials and devices to improve tissue function.[11−19] Traditionally, materials intended to deliver or record electrical signals are made of brittle materials commonly used in the semiconductor industry. However, these materials, including metals and silicon are orders of magnitude stiffer than human tissues, and this mechanical mismatching can lead to inflammation, scar formation, and ultimately device failure. This has inspired efforts to design flexible electroconductive materials to interface with human tissues.[20] Hydrogels are advantageous for many biomedical applications due to their ability to mimic the physical and hydrostatic properties of native tissues, improving the compatibility of implanted devices and materials.[21,22] However, most hydrogels possess poor electrical properties due to the nature of the chemical building blocks used and resultant polymer network that is formed. Another challenge is that engineered electroconductive hydrogels have often been met with limited biocompatibility and/or biodegradability.[12,23,24] For example, incorporating conductive dopant materials such as copper into polyacrylamide hydrogels enhanced bulk material conductivity, yet copper is cytotoxic to several mammalian cell types.[25] Composites containing nonbiodegradable conductive materials such as carbon nanotubes could leave cytotoxic residues or induce fibrosis in the tissue following the digestion of biodegradable components.[26,27]

Conductive polymers (CPs) are a favorable alternative to metallic or carbon-based conductive materials for many biomedical applications due to their versatility and enhanced biocompatibility.[13,28] Unlike many conductive materials, these CPs can be tailored for aqueous dispersion with minor losses in conductivity, which is crucial for biological applications. In addition, CPs contract in the presence of an electric field, which broadens their applications for electrochemical actuation and drug delivery.[29,30] For example, on-demand release of biotinylated nerve growth factor (NGF) was achieved by controlled electrical pulses when loaded onto films of polypyrrole (PPy).[31] Other CPs, CP composites, and CP-carbon nanotube (CNT) composites have been explored for their use as actuators, such as polyaniline (PANI), PANI-CNT, and PPy-PANI.[32] However, most CPs are nonbiodegradable, hydrophobic, and have chemical properties that do not accurately mimic those of the native extracellular matrix (ECM). On the other hand, PEDOT:PSS has been reported as a CP-based biomaterial for bone regeneration,[33] it is easily dispersed in aqueous solutions, it maintains a significant amount (~80%) of its conductive properties in physiological conditions,[34] and is expected to be cleared by the renal system in the body.[35] In addition, although long-term toxicity and biodegradation studies are required to validate PEDOT:PSS as an implantable material, short-term *in vivo* studies involving polyethylene glycol (PEG)-PEDOT:PSS particles have demonstrated that it did not induce toxicity in mice and had a long blood circulation half-life.[36] Although PEDOT:PSS is conductive by itself,[37] it does not contain bioactive ligands and does not form hydrogels alone.

Gelatin methacryloyl (GelMA) hydrogels are derived from collagen, the most abundant protein in the body, and have been shown to support the growth of a range of cell types seeded within or on their structures.[38] The methacryloyl functionalization of gelatin imparts crosslinking ability in the presence of a photoinitiator, allowing for tunable structural and physical properties and rapid gelation kinetics.[38] In addition to tunable physical properties, the arginine-glycine-aspartic acid (RGD) motifs that are present along the peptide backbone in gelatin promote cell attachment and spreading via integrin binding, providing opportunities to utilize it for applications that require direct interaction with cells.[39,40] Both the amide bonds in the peptide chain and the bonds responsible for crosslinking are susceptible to hydrolytic degradation under physiological conditions. Ease of synthesis and versatility has made GelMA one of the most commonly used materials to form hydrogels for biomedical applications.[38]

DOI: 10.1021/acsbiomaterials.8b00135
ACS Biomater. Sci. Eng. 2018, 4, 1558−1567

Here we report on the preparation of hydrogels with tunable electrical, physical, and biological properties. We leverage the bioactive and photosensitive properties of GelMA (Figure 1a) with the conducting properties of a water-dispersible conducting polymer complex, PEDOT:PSS (Figure 1b), to form mechanically flexible and electroconductive hydrogels with tunable properties. Various concentrations of PEDOT:PSS (0, 0.1, 0.3% w/v) were mixed with GelMA prepolymer solution and sonicated to disperse the conductive component throughout the prepolymer solution before crosslinking (Figure 1c, d). To evaluate the potential of these composite hydrogels for biomedical applications, we investigated their mechanical and electrical properties, swelling ratio, and *in vitro* degradation rate. Further, the material was utilized to encapsulate C2C12 myoblasts to evaluate its *in vitro* cytocompatibility.

2. EXPERIMENTAL SECTION

2.1. Materials. Gelatin from cold water fish skin, methacrylic anhydride, 2-hydroxy-4′-(2-hydroxyethoxy)-2-methylpropiophenone (Irgacure 2959) and gold-coated glass slides with a titanium adhesive layer and 100 nm gold coating were purchased from Sigma-Aldrich (St Louis, MO, USA). Dulbecco's modified phosphate buffer saline (DPBS) with no calcium or magnesium was purchased from GE Healthcare Life Sciences (Logan, Utah). PEDOT:PSS was in the form of an aqueous dispersion called Clevios PH 1000 and was purchased from Heraeus (Hanau, Germany). Calcein AM and Ethidium homodimer-1 for live/dead assay and DAPI and Phalloidin conjugated to AlexaFluor 488 for actin/DAPI assay were purchased from Invitrogen (Carlsbad, CA). An Omnicure S2000 UV illumination system from Excelitas Technologies (Waltham, MA) equipped with a 365 nm filter was used for photo-cross-linking of the precursor solutions.

2.2. Preparation of GelMA/PEDOT:PSS Hydrogels. Photo-cross-linkable GelMA prepolymer with ~80% methacryloyl functionalization degree was first synthesized using a previously reported procedure.[41] Briefly, 10 g of gelatin from cold water fish skin was dissolved in 100 mL of DPBS at 60 °C. Once fully dissolved, 8 mL of methacrylic anhydride (Sigma) was added dropwise to the solution and allowed to homogenize. After 3 h of reaction, 300 mL of preheated DPBS at 60 °C was added to the solution to stop the reaction. This solution was dialyzed against deionized (DI) water in dialysis tubing with molecular weight cutoff (MWCO) of 12−14 kDa for 5 days, with DI water changed twice daily. After dialysis, the GelMA was lyophilized for 4 days to generate a fibrous white foam.

To form the hydrogels, we dissolved 7% (w/v) GelMA prepolymer in DI water containing 0.5% (w/v) photoinitiator, a concentration known to be nontoxic to cells encapsulated within GelMA hydrogels.[42] Commercially available PEDOT:PSS solution (Clevios PH 1000) was also sterile filtered (0.22 μm) to remove large aggregates. The concentration of the solution, after filtering, was found to be 0.959 wt % by drying and weighing. Because PEDOT:PSS tends to aggregate at higher temperatures,[43] the PEDOT:PSS solution was sonicated for 30 min after filtration at 4 °C. PEDOT:PSS was added to solutions of GelMA to make 0.1% and 0.3% of final volume. Control GelMA sample with no PEDOT:PSS was also prepared. Appropriate amounts of 10X DPBS (no calcium, no magnesium) were added to each solution to make the salt content of the final solution to be that of 1X DPBS and the solutions were again sonicated at 4 °C for 30 min to disperse the particles in the prepolymer solution before cross-linking (365 nm at 1.8 mW/cm^2).

2.3. Scanning Electron Microscopy (SEM). Cylindrical samples of 60 μL volume (6.0 mm D × 2.0 mm H) were crosslinked for 200 s with UV light and lyophilized using an Isotemp −80 °C freezer from Fisher Scientific (Hampton, NH) and a FreeZone 4.5 lyophilizer from Labconco (Kansas City, MO). Samples were then sectioned in half with a razor blade and sputter coated with a Pt/Pd alloy. SEM images were obtained on a Hitachi S4800 SEM operating at 3.0 kV and 9−10 mm working distance.

2.4. Particle Size Measurements. GelMA/PEDOT:PSS solutions were prepared as detailed in Section 2.2. The average size and distribution of PEDOT:PSS particles in the liquid prepolymer solutions were measured using a Dynamic Light Scattering (DLS) instrument (Malvern Zetasizer, Westborough, MA). The sizes of the particles from SEM images taken from both 0.1% PEDOT:PSS and 0.3% PEDOT:PSS were measured using ImageJ software (NIH). A total of four images were used for measurements, and 50 particles were measured per image.

2.5. Swelling Ratio. Cylindrical samples (60 μL) were prepared and cross-linked as described in Section 2.2, followed by lyophilization. Dry weights were recorded and the samples were submerged in DPBS and then placed into an incubator at standard culture conditions (37 °C; 5% CO_2). Samples were removed and weighed at different time points (1, 4, 8, 12, and 24 h). The swelling ratio was calculated following the equation: $(W_{wet} - W_{dry})/W_{dry} \times 100\%$, where W_{dry} is the weight after lyophilizing and W_{wet} is after removal from DPBS.

2.6. Degradation and Stability Test. Cylindrical samples were prepared, cross-linked and lyophilized as described above. Dry weights were measured at time point 0, and then samples were submerged in 1× DPBS supplemented with 10% fetal bovine serum (FBS) and incubated at 37 °C. The samples were removed from the solution at different time points of 1, 7, and 14 days, at which point they were rinsed with DI water, lyophilized, and the degraded dry weight was recorded. Degradation was calculated based on their weight loss.

To assess the stability of PEDOT:PSS in GelMA, we measured UV−vis spectra of the DPBS storage media with a SpectraMax M3 plate reader (Molecular Devices, Sunnyvale, CA) up to 14 days of incubation. Hydrogel samples were prepared as outlined in Section 2.2, cut into smaller cylinders with a 3 mm biopsy punch, and placed into wells of a 96-well plate containing 200 μL of DPBS and sealed in Parafilm (Bemis NA, Neenah, WI) to prevent water evaporation when stored at 37 °C. Hydrogel samples were removed from the wells before recording UV−vis spectra and were replaced into their respective wells after taking measurements.

2.7. Mechanical Testing. Tensile testing was performed using an Instron 5944 mechanical tester on 60 μL rectangular hydrogels crosslinked in rectangular molds (13.0 mm L × 5.0 mm W × 0.82 mm H). After cross-linking, gels were swollen in DPBS for 16 h at 37 °C so that they reached maximum swelling ratio before testing. Tensile testing was run at a rate of 1 mm/min until failure. Young's, or elastic modulus, was taken as the slope of the linear portion of the curve from 0 to 10% strain. Ultimate tensile strain was taken as the strain point at which hydrogel samples broke.

Compression testing was performed using an Instron 5944 mechanical tester on 60 μL cylindrical gels crosslinked in cylindrical molds (6.0 mm D × 2.0 mm H). After crosslinking, gels were swollen in DPBS for 16 h at 37 °C so that they reached maximum swelling ratio before testing. Hydrogels were compressed in a bath of DPBS at room temperature at a rate of 1 mm/min until 70% strain to prevent damage to the equipment. Three samples were tested at each concentration of PEDOT:PSS. Compressive modulus was taken as the slope of the linear portion of the curve from 0 to 10%.

2.8. Electrochemical Impedance Spectroscopy (EIS). EIS measurements were performed at room temperature on a CH Instruments (Austin, TX, USA) electrochemical workstation. The apparatus was composed of two 12 mm × 12 mm glass slides coated with 100 nm of gold (Sigma-Aldrich). The electrodes were connected to copper wires with silver paste, and this connection was covered with epoxy resin to prevent tarnishing of the silver. Cylindrical hydrogels (60 μL) were swollen in DI water for 16 h at 37 °C to remove the salt ions present in DPBS. The water was replaced with fresh DI twice in this time. Because hydrogels were swollen overnight and had different sizes after swelling, circular sections of the hydrogels were punched with a 0.8 cm biopsy punch and sandwiched between the gold-coated glass slides. A 0.65 mm polydimethylsiloxane (PDMS) spacer was placed around the gel to maintain a constant distance between the electrodes. The top electrode was then taped down on the spacer to maximize contact between the electrodes and the hydrogel. Measure-

DOI: 10.1021/acsbiomaterials.8b00135
ACS Biomater. Sci. Eng. 2018, 4, 1558−1567

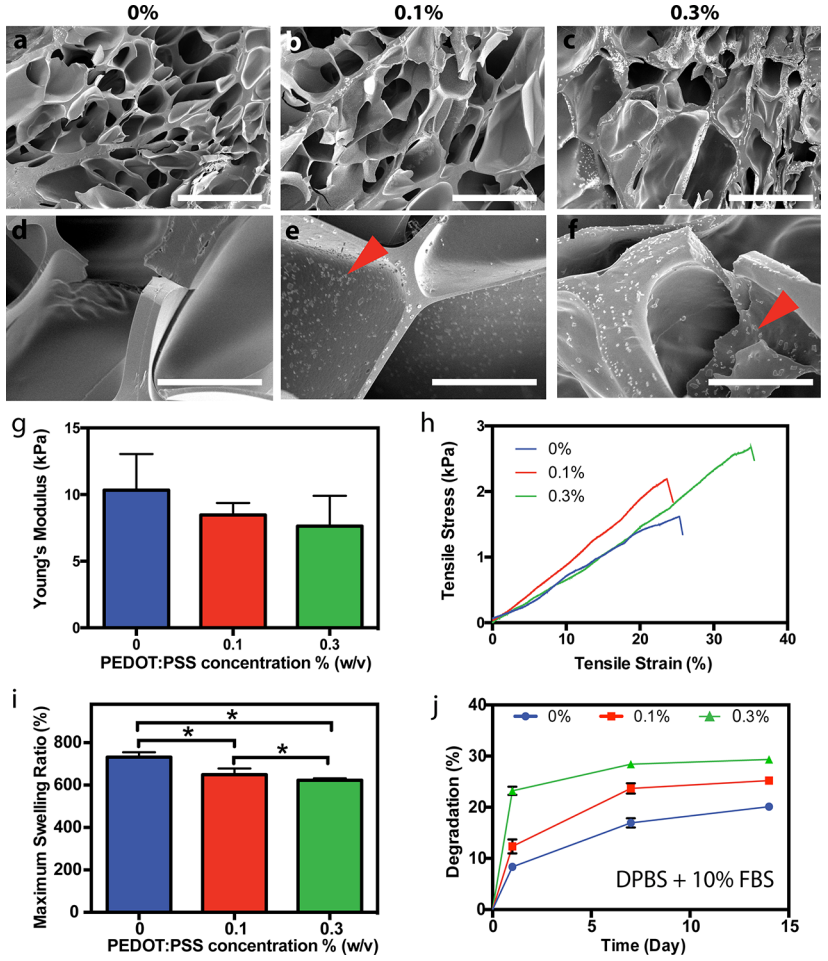

Figure 2. Physical and microstructural characterization of GelMA/PEDOT:PSS hydrogels. Representative SEM images of cross-linked hydrogels at concentrations of (a, d) 0%, (b, e) 0.1% and (c, f) 0.3% PEDOT:PSS (scale bars for a–c = 100 μm; scale bars for d–f = 20 μm). Red arrowheads in e and f indicate the presence of nanoparticles dispersed along and within the pore walls of the hydrogel. (g) Young's modulus of hydrogels cross-linked for 200 s (* = $p < 0.05$). (h) Representative tensile stress–strain curves for hydrogels with varying concentration of PEDOT:PSS. (i) Maximum swelling ratio of hydrogels at varying concentration of PEDOT:PSS (* = $p < 0.05$). (j) Degradation curve of hydrogels with varying concentration of PEDOT:PSS at days 1, 7, and 14 in DPBS supplemented with 10% FBS.

ments were recorded between 0.1 and 100 Hz with an AC amplitude of ±10 mV.

2.9. *Ex Vivo* Tissue Stimulation. Directly after euthanizing rats by exsanguination, the *rectus abdominis* muscle was dissected and sectioned into 0.5 cm × 1.5 cm pieces. Two pieces of tissue were placed at a distance of 1 cm in a PDMS mold, and 150 μL of the precursor was pipetted and cross-linked between them with UV light for 200 s. To test wave propagation through the conductive hydrogel, electrical stimulation was performed on one of the tissue sections using a 3320A 20 MHz Function/Arbitrary Waveform Generator (Agilent, Santa Clara, CA, USA) connected to two platinum wires at 1 Hz pulses with a duration of 50 ms. Voltage was raised from 1 V_{pp} until both pieces of tissue connected with the hydrogel visually contracted. The excitation threshold was taken as the minimum voltage required to induce contraction of the explanted tissue.

2.10. Cell Encapsulation. C2C12 cells (ATCC CRL1772) were cultured under standard conditions (37 °C; 5% CO_2) with Dulbecco's modified Eagle medium (DMEM) supplemented with 10% fetal bovine serum and 1% penicillin/streptomycin (Life Technologies).

To form cell-laden hydrogels, we prepared 7% hydrogel precursor solution as previously described (Section 2.2), but media was used as the solvent under sterile conditions. Cells were detached using trypsin-EDTA (0.25% v/v), centrifuged, and resuspended in the precursor solution at 10 million cells/mL before cross-linking. The precursor/cell solution (7 μL) was sandwiched on a Petri dish between two 150 μm spacers. A 3-(trimethoxysilyl)propyl methacrylate (TMSPMA) coated glass slide was then placed on top of the solution and placed in a UV box to be cross-linked. Exposure time varied between 25 and 30 s, depending on the concentration of PEDOT:PSS. Samples were cultured in 24 well plates with 400 μL of media. Media was changed twice in the first 30 min after cross-linking to remove unreacted photoinitiator, and subsequently changed daily. Live/Dead and Actin/DAPI assays were performed on days 1, 3, and 5. Fluorescence imaging was performed on an Axio Observer Z1 inverted microscope (Carl Zeiss, Oberkochen, Germany). Cell viability was quantified using ImageJ software (NIH) from Live/Dead images.

For Live/Dead assay, cells were stained with calcein AM (live) or ethidium homodimer-1 (dead) and incubated for 15 min. After staining, scaffolds were washed with DPBS three times and wells were filled with 400 μL of DPBS before imaging. For Actin/DAPI assay, cells were fixed in 4% paraformaldehyde for 45 min and washed three times with DPBS with 5 min intervals between washes. This was followed by permeabilization with 0.1% Triton X-100 in DPBS for 20 min. Filamentous actin was stained with AlexaFluor 488 conjugated to Phalloidin for 45 min and washed three times with DPBS, followed by staining of the cell nuclei with DAPI for 5 min and three washes with DPBS. Fluorescent images were obtained on an inverted microscope (Zeiss Axio Observer Z1).

2.11. Statistical Analysis. All experiments were performed at least in triplicate, and data are presented as mean ± standard deviation (SD). Statistical analysis was performed in GraphPad Prism software.

DOI: 10.1021/acsbiomaterials.8b00135
ACS Biomater. Sci. Eng. 2018, 4, 1558–1567

One-way ANOVA tests were performed to determine statistical significance, and P values less than 0.05 were considered as significant.

3. RESULTS AND DISCUSSION

3.1. Physical and Microstructural Characterization of Composite Hydrogels. SEM images of pure GelMA (Figure 2a, d) and composite GelMA/PEDOT:PSS (Figure 2b, c, e, f) hydrogels revealed the presence of homogeneously distributed particles both embedded in, and adsorbed onto the hydrogel pore walls (Figure 2e, f) but not in pristine GelMA hydrogels (Figure 2d), which showed smooth pore walls. The presence of these particles throughout the composite materials correlated well with the hydrogel's homogeneous opaque color (Figure 1d) and electrical properties, which is attributed to PEDOT:PSS. In addition, particle size measurement before cross-linking (using DLS) and after cross-linking (using SEM) suggest that the particles observed correspond most likely to PEDOT:PSS particles. The average particle size of the strongest peak of DLS measurements before cross-linking was 209.0 ± 19.6 nm, and represents approximately 82% of the particles in the spectrum (Figure S1a). Approximately 94% of particles measured from SEM images were in the range of 100−500 nm, with a distribution centered at 243.6 nm (Figure S1b). A representative SEM image at high magnification that was used to measure particle size is shown in Figure S1c. The DLS and SEM sizes are within experimental error and are thus evidence that the particles in SEM images are likely dispersed aggregates of PEDOT:PSS. Patton et al. dispersed PEDOT:PSS within a poly(vinyl alcohol) (PVA) hydrogel that showed visible phase separation at low concentrations of PEDOT:PSS, where the particles preferentially aggregated in the center of the resulting hydrogels.[44] This phenomenon was not observed herein, suggesting homogeneous distribution of the conductive material in the GelMA network and their immobilization within the hydrogel, which may be due to the repeated cycles of sonication prior to photopolymerization.

Photo-crosslinked hydrogel systems enable precise control over the mechanical properties simply by varying light exposure time, and prepolymer and photoinitiator concentrations.[45] In particular, GelMA-based hydrogel formulations have been tuned to exhibit compressive moduli ranging from 1 to 100 kPa to mimic the properties of different tissues.[38,46] Similar to previous reports, the compressive modulus of our composite hydrogels increased with crosslinking time from 100 to 200 s (Figure S2a). In addition, we found that compressive modulus decreased slightly with the loading fraction of PEDOT:PSS (Figure S2b) from 3.6 ± 0.1 kPa for pure GelMA to 3.1 ± 0.2 kPa and 2.7 ± 0.06 kPa for hydrogels containing 0.1% (w/v) and 0.3% (w/v) PEDOT:PSS, respectively, when exposed to UV light for 200 s. Although the bulk compressive modulus of our samples decreased slightly with increasing PEDOT:PSS concentration, we noted that at higher strain level, in the densification portion of the stress/strain curves (indicated by the arrow in Figure S3a), the hydrogels containing PEDOT:PSS possessed a higher stress when compared to pristine GelMA hydrogels. In this later region of the stress/strain curves (at 40−50% strain level), the modulus for composite hydrogel containing 0.3% PEDOT:PSS was 1.4-fold higher than pristine GelMA hydrogels (Figure S3b). This may be due to the strong interactions of PEDOT:PSS with guanidinium groups of arginine in the gelatin backbone,[47] as well as contacts between the pore walls containing rigid PEDOT:PSS particles as the hydrogels were compressed. Furthermore, results of tensile testing for the composite hydrogels yielded Young's moduli ranging from 7.6 ± 2.3 kPa to 10.3 ± 2.7 kPa with no significant difference among tested materials containing different concentration of PEDOT:PSS (Figure 2g). However, hydrogel samples containing 0.3% PEDOT:PSS also exhibited significantly higher ultimate tensile strain compared to other concentrations tested (Figure S4). This enhanced extensibility could be due to electrostatic interactions between PSS and the gelatin backbone, resulting in reversible bonding in the composite system and a more stretchable network. Representative stress−strain curves from tensile testing of the hydrogel samples are shown in Figure 2h.

Swelling ratio have significant effects on the volume, mechanical properties, molecular diffusion and ultimately the integration of hydrogels with surrounding tissues.[48,49] In our study, the swelling ratio was found to decrease from 731.8 ± 23.2% for pure GelMA hydrogels to 648 ± 29.4% and 622.5 ± 9.30% for composite hydrogels containing 0.1% and 0.3% PEDOT:PSS, respectively (Figure 2i) after 24 h in DPBS. All hydrogels reached their maximum swelling ratio after 8 h of incubation in DPBS at 37 °C (Figure S5). In addition, our results showed that the *in vitro* hydrolytic degradation rates at early time points (day 1) of the composite hydrogels increased concomitantly from 11.8 ± 2.1% for pure GelMA to 16.2 ± 0.8% and 24.1 ± 3.2% for 0.1% and 0.3% PEDOT:PSS, respectively (Figure 2j). However, the degradation rate leveled out quickly for hydrogels containing PEDOT:PSS. The observed lower swelling ratio and increased early degradation for composite hydrogels might be a result of a slightly lower degree of crosslinking in the samples containing PEDOT:PSS particles, causing un-crosslinked GelMA to diffuse from the matrix. Possible explanations for these results could be reduced light penetration in the samples, or cross-reactivity of the radical with the conjugated polymer, PEDOT. As earlier reports have shown that the presence of PEDOT:PSS (1.3% w/v) increased light scattering and decreased transmittance at 550 nm from >90% to 70% as thin film thicknesses increase from 50 to 300 nm, this observation may be more likely as a result of decreased light penetration in the samples containing PEDOT:PSS.[50] On the other hand, GelMA polymerization and hydrogel formation usually take place on the order of seconds or minutes,[42,51] whereas PEDOT polymerization normally requires hours or days, even in the presence of a radical.[52,53] This suggests that the kinetics of radical polymerization of GelMA are much faster than radical polymerization of PEDOT, and there is likely little reactivity of the radical initiator with PEDOT.

Because the PEDOT:PSS particles in this study were simply dispersed in the GelMA hydrogels, we sought to determine if the conductive particles would leach out into surrounding media as the network degraded, which would ultimately diminish the conductivity of the bulk material. UV−vis absorbance measurements were taken of DPBS storage solutions surrounding the hydrogels during a degradation study to determine if PEDOT:PSS was diffusing out of the hydrogels. An increased absorbance of the saline in wavelengths ranging from ∼400−1000 nm would signify a higher content of PEDOT:PSS in the saline (Figure S6a), indicating significant diffusion of PEDOT:PSS from the crosslinked matrix. However, for hydrogels containing PEDOT:PSS, we observed very minor change in the absorbance spectra (Figure S6c, d). The increased absorbance in the DPBS solution surrounding GelMA hydrogels corresponds to degraded GelMA polymer

DOI: 10.1021/acsbiomaterials.8b00135
ACS Biomater. Sci. Eng. 2018, 4, 1558−1567

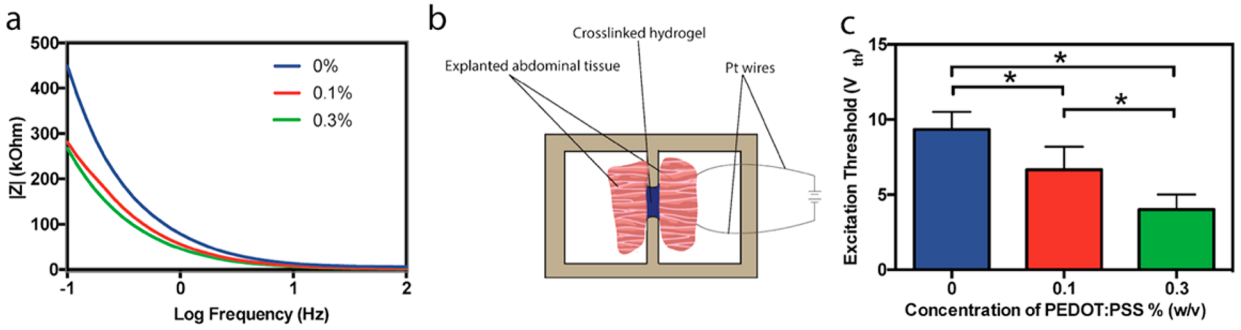

Figure 3. Electrical characterization of GelMA/PEDOT:PSS hydrogels. (a) Electrochemical impedance spectroscopy (EIS) measurements of hydrogels containing various concentrations of PEDOT:PSS. (b) Schematic showing setup for *ex vivo* abdominal tissue stimulation. (c) Excitation threshold voltage (V_{th}) required to stimulate severed pieces of abdominal tissue from Wistar rats, connected by hydrogels containing 7% GelMA with various concentrations of PEDOT:PSS (* = $p < 0.05$).

fragments, as this increase corresponds with the absorbance of GelMA precursor (Figure S6b). These data suggest that the hydrogels containing PEDOT:PSS might be chemically more stable to degradation than those without it, possibly due to PEDOT:PSS particles preventing hydrolysis of ester and amide groups in the hydrogel network.

3.2. Conductivity Characterization. Ion transport in electroactive tissues naturally occurs at a range of frequencies and in a bidirectional, alternating fashion. Thus, impedance spectroscopy, which accounts for electron transfer from capacitive and resistive effects, was implemented for measuring the electrical properties of biomaterials for interfacing with living tissue.[54] All the hydrogels investigated exhibited low impedance at high applied frequencies, as shown in Figure 3a, due to capacitive currents in the gels.[55] At lower frequencies similar to those in electroactive biological tissues (1 Hz), resistive currents dominate and composite hydrogels containing 0.1% and 0.3% PEDOT:PSS possessed lower impedance than pure GelMA hydrogel. At 1 Hz frequency, the impedance decreased from 449.0 kOhm for plain GelMA to 281.2 kOhm and 261 kOhm for hydrogels containing 0.1 and 0.3% PEDOT:PSS, respectively. These results confirmed the enhanced electroconductivity of the hydrogels containing PEDOT:PSS.

The ability of an implanted material to conduct current between biological specimens is a major objective in the design of electroconductive biomaterials. To test this capability for our composite hydrogels, abdominal muscle tissue was explanted from Wistar rats after euthanasia. An AC electrical bias was applied to one piece of tissue at varying voltage using platinum wires connected to a pulse generator until both tissue fragments contracted, as previously reported (Figure 3b).[11] This setup resulted in brief contractions of the explanted tissue at a low enough frequency such that they could be visually observed. The observable excitation threshold required to induce tissue contraction decreased from 9.3 ± 1.2 V to 6.7 ± 1.5 V and 4.0 ± 1.0 V as the concentration of PEDOT:PSS incorporated in the hydrogel was increased from 0% to 0.1% and 0.3%, respectively (Figure 3c, Movie S1). This decrease in excitation threshold was more profound than what was previously reported for a composite hydrogel of tropoelastin and graphene oxide (GO),[11] wherein increasing the concentration of GO from 0 to 1 mg/mL (0.1% w/v) resulted in a decrease in threshold voltage from ∼5.8 to ∼3.9 V. In summary, these results demonstrate the ability of the GelMA/PEDOT:PSS hydrogel to receive and transmit electrochemical signals from living tissue.

3.3. Cell Encapsulation in 3D GelMA/PEDOT:PSS Conductive Hydrogels. Despite their ultrahigh conductivity, dopants for increasing conductivity of biomaterials such as graphene and single-walled CNTs have been plagued with aggregation in aqueous media, long retention time *in vivo*, and inflammation.[56,57] To evaluate the cytocompatibility of our engineered conductive biomaterial, C2C12 myoblast cells were encapsulated within all formulations of the GelMA/PEDOT:PSS hydrogels. Myoblasts were selected to evaluate cytocompatibility because they are commonly used in studies of conductive materials for biomedical applications.[54,58,59] Cell-laden gels with 150 μm thickness were formed on TMSPMA-coated glass slides via chemical bonding between GelMA and TMSPMA. Metabolically active cells are generally located at 40−200 μm from the nearest capillary, so nutrient deficiency was not expected to contribute to cell viability.[60] In addition, thin films of hydrogel prepolymer require shorter crosslinking times that are not harmful to cells. Therefore, a constant cell-laden gel thickness of 150 μm was maintained to increase nutrient diffusion and minimize cell exposure to UV light. The high cell viability observed in Figures 4b, e confirmed that the incorporation of 0.1% PEDOT:PSS did not significantly affect cell viability on both days 1 and 5 as compared to control sample without PEDOT:PSS (Figures 4a, d). However, the addition of 0.3% PEDOT:PSS exhibited a lower cell viability (Figures 4c, f). Live/Dead images from day 3 showed a similar trend (Figure S7a−c). The quantification of viability (Figure 4m) demonstrated that cell viability was above 77% in all hydrogel formulations up to day 3. However, viability dropped at day 5 to 35.5 ± 12.1% for cells encapsulated in 0.3% PEDOT:PSS.

Cell morphology was determined by Actin/DAPI staining (Figure 4g−l). Actin/DAPI images at day 3 showed a similar trend as those at days 1 and 5 (Figure S7d−f). Cell spreading, defined as the area of cell clusters divided by the number of cell nuclei within those clusters, was similar for GelMA and GelMA containing 0.1% PEDOT:PSS samples throughout 5 days of culture. However, for hydrogels containing 0.3% PEDOT:PSS, cell spreading was significantly lower on days 1, 3, and 5 of culture. For example, cell spreading was 361.6 ± 137.8 μm^2 in GelMA/0.3% PEDOT:PSS on day 1, which was 2.3-fold lower than pristine GelMA (830.5 ± 334.0 μm^2) (Figure 4n).

The decrease in viability and spreading for the cells encapsulated in the highest concentration of PEDOT:PSS is

DOI: 10.1021/acsbiomaterials.8b00135
ACS Biomater. Sci. Eng. 2018, 4, 1558−1567

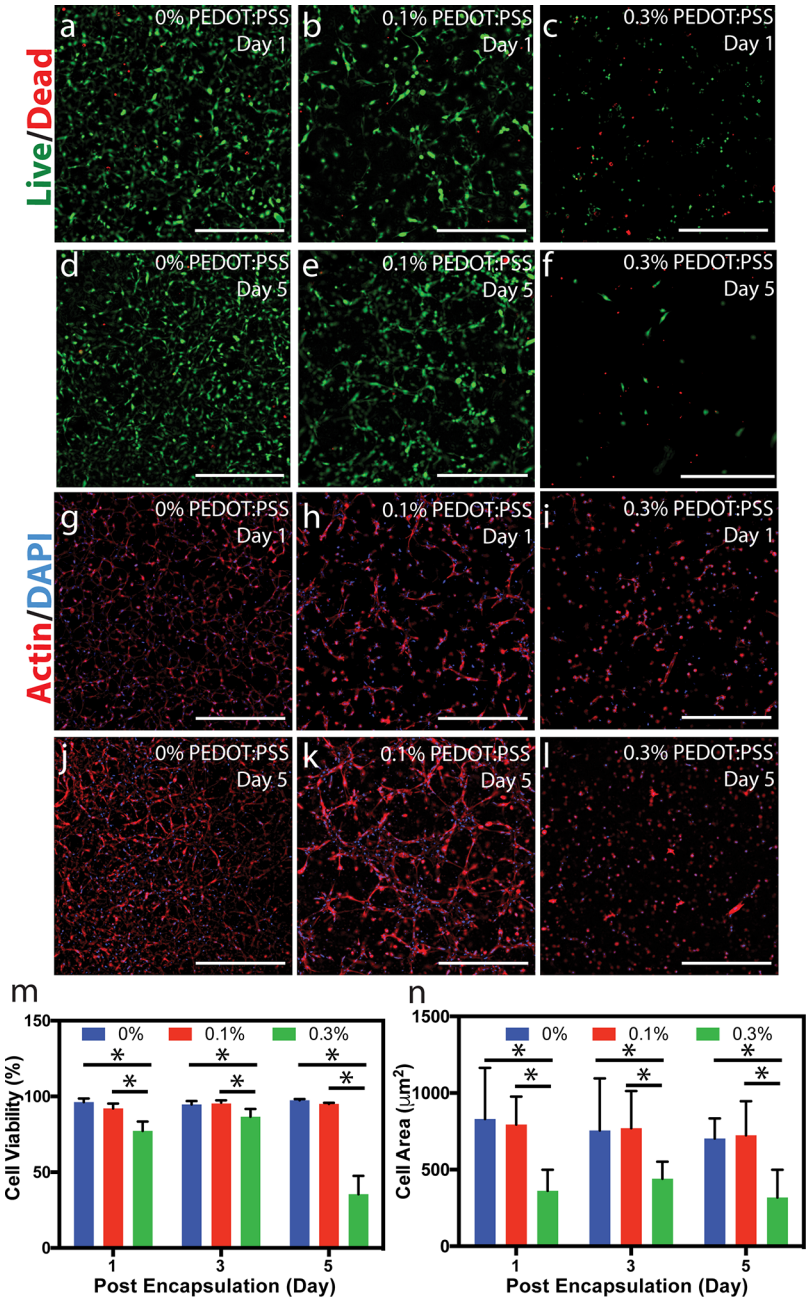

Figure 4. 3D cell encapsulation in GelMA/PEDOT:PSS hydrogels. Representative Live/Dead images from C2C12 cells encapsulated in (a, d) 0, (b, e) 0.1, and (c, f) 0.3% PEDOT:PSS over 5 days of culture (scale bars = 500 μm). Representative Actin/DAPI images from C2C12 cells encapsulated in (g, j) 0, (h, k) 0.1, and (i, l) 0.3% PEDOT:PSS over 5 days of culture (scale bars = 500 μm). (m) Quantification of viability for cells encapsulated in GelMA hydrogels containing varied concentration of PEDOT:PSS at different days (* = $p < 0.05$).(n) Quantification of cell spreading, defined as the area of cell clusters divided by the number of cells within those clusters, for cells encapsulated in GelMA hydrogels containing varied concentration of PEDOT:PSS at different days (* = $p < 0.05$).

likely due to the anionic environment in the hydrogels that was imparted by adding PEDOT:PSS. Specifically, the anionic PSS chain (2.5× more abundant by weight than PEDOT in our dispersion) may have limited cell attachment and, as a result, created a less favorable environment for cell survival. Ai et al. showed that cells cultured on a film of PSS were less viable than those cultured on gelatin films.[61] Cell attachment is normally favored in gelatin via integrin binding since RGD groups, as well as lysine groups, are available as a result of the denaturing process.[62,63] We hypothesize that larger amounts of PSS may limit RGD accessibility due to strong electrostatic interactions between PSS and the guanidinium groups of arginine amino acids in RGD.[47] In addition, lysine groups, which also promote cell attachment, are also altered via methacrylation of gelatin,[42] and thus add to the lower availability of cationic sites for cell attachment. Previous investigations have confirmed the necessity of RGD in protein-based materials for cell attachment by comparing attachment and spreading of cells encapsulated in or seeded on hydrogels containing the proper RGD sequence with a scrambled RDG.[64−66] At lower concentrations of PEDOT:PSS, attachment and spreading are still favored, and indicate that fewer arginine groups are bound to PEDOT:PSS

DOI: 10.1021/acsbiomaterials.8b00135
ACS Biomater. Sci. Eng. 2018, 4, 1558−1567

particles. Our future experiments will focus on studying the effect of calcium chloride on cell attachment in GelMA/PEDOT:PSS hydrogels. For certain biomedical applications, such as those that require the delivery of cell-laden conductive scaffolds, hydrogels containing 0.1% PEDOT:PSS may have appropriate mechanical properties, enhanced conductivity compared to pristine GelMA hydrogel, and a high degree of cytocompatibility. However, *in vivo* tests are required to determine the foreign body response, regenerative capability, and clearance of PEDOT:PSS particles to validate the potential of our composite hydrogel as an implantable cell-laden material for applications such as tissue regeneration.

Typical chemical crosslinking methods used for engineering conductive hydrogels or scaffolds can be toxic to cells and/or require long times, some on the order of days,[12,35] such that cell encapsulation within these hydrogels is difficult or impossible. For example, crosslinking of a single-component polythiophene hydrogel was performed in dimethyl sulfoxide (DMSO) in the presence of 1,1′-carbonyldiimidazole (CDI), both of which are toxic to cells, and gelation took 2 days.[12] For this reason, 2D cell experiments, in which cells are seeded on top of the scaffold after complete crosslinking and/or washing, are commonly reported. While these materials may be suitable for a range of applications, 3D cell encapsulation is more informative in determining the biocompatibility and performance of a scaffold for a particular application, as it closely mimics the 3D biological microenvironment that cells are exposed to *in vivo*.[67] This biological microenvironment is tissue-specific and includes chemical and mechanical cues, cell−cell contacts and signaling, nutrient and metabolic byproducts circulation.[68,69] In this report, encapsulation of cells within photo-crosslinkable and conductive gels was accomplished with relatively short crosslinking times. Furthermore, our scaffold is mainly composed of denatured collagen, and is thus better representative of the structural collagen matrix present in many soft tissues. Although we observed limited viability at the highest concentration of PEDOT:PSS that was tested, we believe efforts to neutralize charges on the PSS chain using self-assembled rosette nanotubes, for example,[40,70−75] will improve cell viability and mechanical stiffness.

4. CONCLUSIONS

The synthesis of conductive hydrogels for biomedical applications and cellular interfacing is still met with a number of challenges, including limited biocompatibility, biodegradability, and dispersion of dopant materials in hydrophilic prepolymer solutions. Combining the advantageous properties of hydrogels with the tunable properties of CPs may overcome some of these challenges and generate multifunctional biomaterials for a range of applications. Here, electroconductive composite hydrogels stable under physiological conditions were synthesized by combining two readily available materials, a CP (PEDOT:PSS) with a biologically derived polymer (GelMA). Physical properties of the resulting hydrogel, such as swelling, degradation, and mechanics were modulated by changing the concentration of CP incorporated within the hydrogel network. The doped hydrogels showed lower impedance than nondoped GelMA controls at physiologically relevant frequencies and enabled excitation of abdominal muscle tissue via charge potential transferred through the electroconductive[76] hydrogel. In this study, enhanced conductivity and biocompatibility up to a concentration of 0.1% PEDOT:PSS, as well as moderate degradation rate and comparable mechanics to pristine GelMA hydrogels, were shown. Impedance spectroscopy results indicate that hydrogels containing 0.1% and 0.3% PEDOT:PSS have comparable impedance, and thus increasing the concentration of PEDOT:PSS to 0.3% is unnecessary to improve electrical properties, as cell viability decreased drastically for cells encapsulated in these hydrogels 5 days post encapsulation. This hydrogel system may have utility in applications where a soft, flexible, and conductive material capable of interfacing with human tissues is needed, such as on-skin electrodes or neural probes.

■ ASSOCIATED CONTENT

Supporting Information

The Supporting Information is available free of charge on the ACS Publications website at DOI: 10.1021/acsbiomaterials.8b00135.

Figure S1, characterization of particle size in GelMA/PEDOT:PSS composites; Figure S2, compressive testing of cylindrical hydrogels; Figure S3, modulus of GelMA/PEDOT:PSS hydrogels at high compressive strain; Figure S4, ultimate tensile strain of hydrogels with varying PEDOT:PSS loading; Figure S5, swelling ratio of GelMA/PEDOT:PSS hydrogels at various time points; Figure S6, UV−vis spectra of degradation solutions; Figure S7, representative fluorescence microscopy images from 3D cell encapsulation (PDF)

Movie S1, *ex vivo* stimulation of abdominal tissue (MOV)

■ AUTHOR INFORMATION

Corresponding Authors

*E-mail: h.fenniri@neu.edu. Tel: (617) 373-7690.
*E-mail: n.annabi@neu.edu. Tel: (617) 373-5350.

ORCID

Hicham Fenniri: 0000-0001-7629-7080

Author Contributions

The manuscript was written through contributions of all authors. All authors have given approval to the final version of the manuscript.

Funding

American Heart Association, Grant 16SDG31280010; Interdisciplinary Research Seed Grants from Northeastern University, Grant FY17 TIER 1; National Institutes of Health, Grants R01-EB023052 and R01HL140618.

Notes

The authors declare no competing financial interest.

■ ACKNOWLEDGMENTS

The authors acknowledge the support from Northeastern University, and the startup fund provided by the Department of Chemical Engineering, College of Engineering at Northeastern University. Also, N.A. acknowledge the support from the American Heart Association (AHA, 16SDG31280010) and the National Institutes of Health (R01-EB023052; R01HL140618). The authors also acknowledge Robert Eagan for assistance with the setup for *ex vivo* tissue stimulation, Ehsan Shirzaei Sani and William Fowle for assistance with SEM, William Fowle for the setup for electrochemical impedance spectroscopy, and Dr. Su-Ryon Shin for assistance with electrochemical impedance spectroscopy.

DOI: 10.1021/acsbiomaterials.8b00135
ACS Biomater. Sci. Eng. 2018, 4, 1558−1567

REFERENCES

(1) Nagamine, K.; Chihara, S.; Kai, H.; Kaji, H.; Nishizawa, M. Totally shape-conformable electrode/hydrogel composite for on-skin electrophysiological measurements. *Sens. Actuators, B* **2016**, *237*, 49−53.

(2) Bishay, J. M.; Janae, C. Independently deployable sealed defibrillator electrode pad and method of use. European Patent EP0983775A2, 2001.

(3) Rolf, D. Medical electrode for monitoring and diagnostic use. U.S. Patent 4 674 512, 1987.

(4) Heo, D. N.; Song, S.-J. J.; Kim, H.-J. J.; Lee, Y. J.; Ko, W.-K. K.; Lee, S. J.; Lee, D.; Park, S. J.; Zhang, L. G.; Kang, J. Y.; Do, S. H.; Lee, S. H.; Kwon, I. K. Multifunctional hydrogel coatings on the surface of neural cuff electrode for improving electrode-nerve tissue interfaces. *Acta Biomater.* **2016**, *39*, 25−33.

(5) Yang, J.; Kim, D. H.; Hendricks, J. L.; Leach, M.; Northey, R.; Martin, D. C. Ordered surfactant-templated poly(3,4-ethylenedioxythiophene) (PEDOT) conducting polymer on microfabricated neural probes. *Acta Biomater.* **2005**, *1* (1), 125−136.

(6) Zhang, D.; Di, F.; Zhu, Y.; Xiao, Y.; Che, J. Electroactive hybrid hydrogel: Toward a smart coating for neural electrodes. *J. Bioact. Compat. Polym.* **2015**, *30* (6), 600−616.

(7) Ge, J.; Neofytou, E.; Cahill, T. J. I.; Beygui, R. E.; Zare, R. N. Drug Release from Electric-Field-Responsive Nanoparticles. *ACS Nano* **2012**, *6* (1), 227−233.

(8) O'Grady, M. L.; Kuo, P.-l.; Parker, K. Optimization of Electroactive Hydrogel Actuators. *ACS Appl. Mater. Interfaces* **2010**, *2* (2), 343−346.

(9) Hoang, P.; Phung, H.; Nguyen, C.; Dat Nguyen, T.; Choi, H. A highly flexible, stretchable and ultra-thin piezoresistive tactile sensor array using PAM/PEDOT:PSS hydrogel. *2017 14th International Conference on Ubiquitous Robots and Ambient Intelligence (URAI)* **2017**, 950−955.

(10) Mehrali, M.; Thakur, A.; Pennisi, C.; Talebian, S.; Arpanaei, A.; Nikkhah, M.; Dolatshahi-Pirouz, A. Nanoreinforced Hydrogels for Tissue Engineering: Biomaterials that are Compatible with Load Bearing and Electroactive Tissues. *Adv. Mater.* **2017**, *29*, 1603612.

(11) Annabi, N.; Shin, S.; Tamayol, A.; Miscuglio, M.; Bakooshli, M.; Assmann, A.; Mostafalu, P.; Sun, J. Y.; Mithieux, S.; Cheung, L.; Tang, X.; Weiss, A. S.; Khademhosseini, A. Highly Elastic and Conductive Human-Based Protein Hybrid Hydrogels. *Adv. Mater.* **2016**, *28*, 40.

(12) Mawad, D.; Stewart, E.; Officer, D. L.; Romeo, T.; Wagner, P.; Wagner, K.; Wallace, G. G. A Single Component Conducting Polymer Hydrogel as a Scaffold for Tissue Engineering. *Adv. Funct. Mater.* **2012**, *22* (13), 2692−2699.

(13) Guimard, N. K.; Gomez, N.; Schmidt, C. E. Conducting polymers in biomedical engineering. *Prog. Polym. Sci.* **2007**, *32* (8), 876−921.

(14) Green, R. A.; Hassarati, R. T.; Goding, J. A.; Baek, S.; Lovell, N. H.; Martens, P. J.; Poole-Warren, L. A. Conductive Hydrogels: Mechanically Robust Hybrids for Use as Biomaterials. *Macromol. Biosci.* **2012**, *12* (4), 494−501.

(15) You, J. O.; Rafat, M.; Ye, G. J. C.; Auguste, D. T. Nanoengineering the heart: conductive scaffolds enhance connexin 43 expression. *Nano Lett.* **2011**, *11*, 3643.

(16) Wu, Y.; Wang, L.; Guo, B.; Shao, Y.; Ma, P. X. Electroactive biodegradable polyurethane significantly enhanced Schwann cells myelin gene expression and neurotrophin secretion for peripheral nerve tissue engineering. *Biomaterials* **2016**, *87*, 18−31.

(17) Xie, M.; Wang, L.; Ge, J.; Guo, B.; Ma, P. X. Strong electroactive biodegradable shape memory polymer networks based on star-shaped polylactide and aniline trimer for bone tissue engineering. *ACS Appl. Mater. Interfaces* **2015**, *7* (12), 6772−6781.

(18) Wu, Y.; Wang, L.; Guo, B.; Ma, P. X. Interwoven Aligned Conductive Nanofiber Yarn/Hydrogel Composite Scaffolds for Engineered 3D Cardiac Anisotropy. *ACS Nano* **2017**, *11*, 5646.

(19) Chen, J.; Dong, R.; Ge, J.; Guo, B.; Ma, P. X. Biocompatible, Biodegradable, and Electroactive Polyurethane-Urea Elastomers with Tunable Hydrophilicity for Skeletal Muscle Tissue Engineering. *ACS Appl. Mater. Interfaces* **2015**, *7* (51), 28273−28285.

(20) Rivnay, J.; Wang, H.; Fenno, L.; Deisseroth, K.; Malliaras, G. G. Next-generation probes, particles, and proteins for neural interfacing. *Science Advances* **2017**, *3* (6), e1601649.

(21) Annabi, N.; Nichol, J. W.; Zhong, X.; Ji, C.; Koshy, S.; Khademhosseini, A.; Dehghani, F. Controlling the Porosity and Microarchitecture of Hydrogels for Tissue Engineering. *Tissue Eng., Part B* **2010**, *16* (4), 371−380.

(22) Spencer, K. C.; Sy, J. C.; Ramadi, K. B.; Graybiel, A. M.; Langer, R.; Cima, M. J. Characterization of Mechanically Matched Hydrogel Coatings to Improve the Biocompatibility of Neural Implants. *Sci. Rep.* **2017**, *7* (1), 1952.

(23) Dai, T.; Jiang, X.; Hua, S.; Wang, X.; Lu, Y. Facile fabrication of conducting polymer hydrogels via supramolecular self-assembly. *Chem. Commun.* **2008**, *0* (36), 4279−4281.

(24) Dvir, T.; Timko, B. P.; Brigham, M. D.; Naik, S. R.; Karajanagi, S. S.; Levy, O.; Jin, H.; Parker, K. K.; Langer, R.; Kohane, D. S. Nanowired three-dimensional cardiac patches. *Nat. Nanotechnol.* **2011**, *6* (11), 720−725.

(25) Lin, J.; Tang, Q.; Wu, J. The synthesis and electrical conductivity of a polyacrylamide/Cu conducting hydrogel. *React. Funct. Polym.* **2007**, *67* (6), 489−494.

(26) Shin, S. R.; Jung, S. M.; Zalabany, M.; Kim, K.; Zorlutuna, P.; Kim, S. b.; Nikkhah, M.; Khabiry, M.; Azize, M.; Kong, J.; et al. Carbon-nanotube-embedded hydrogel sheets for engineering cardiac constructs and bioactuators. *ACS Nano* **2013**, *7*, 2369−2380.

(27) Koppes, A. N.; Keating, K. W.; McGregor, A. L.; Koppes, R. A.; Kearns, K. R.; Ziemba, A. M.; McKay, C. A.; Zuidema, J. M.; Rivet, C. J.; Gilbert, R. J.; Thompson, D. M. Robust neurite extension following exogenous electrical stimulation within single walled carbon nanotube-composite hydrogels. *Acta Biomater.* **2016**, *39*, 34−43.

(28) Balint, R.; Cassidy, N. J.; Cartmell, S. H. Conductive polymers: Towards a smart biomaterial for tissue engineering. *Acta Biomater.* **2014**, *10* (6), 2341−2353.

(29) Ma, M.; Guo, L.; Anderson, D. G.; Langer, R. Bio-Inspired Polymer Composite Actuator and Generator Driven by Water Gradients. *Science* **2013**, *339* (6116), 186−189.

(30) Abidian, M. R.; Kim, D. H.; Martin, D. C. Conducting-Polymer Nanotubes for Controlled Drug Release. *Adv. Mater.* **2006**, *18* (4), 405−409.

(31) George, P. M.; LaVan, D. A.; Burdick, J. A.; Chen, C. Y.; Liang, E.; Langer, R. Electrically Controlled Drug Delivery from Biotin Doped Conductive Polypyrrole. *Adv. Mater.* **2006**, *18* (5), 577−581.

(32) Ravichandran, R.; Sundarrajan, S.; Venugopal, J. R.; Mukherjee, S.; Ramakrishna, S. Applications of conducting polymers and their issues in biomedical engineering. *J. R. Soc., Interface* **2010**, *7* (Suppl_5), S559−S579.

(33) Khan, S.; Ul-Islam, M.; Ullah, M.; Kim, Y.; Park, J. Synthesis and characterization of a novel bacterial cellulose-poly(3,4-ethylenedioxythiophene)-poly(styrene sulfonate) composite for use in biomedical applications. *Cellulose* **2015**, *22* (4), 2141−2148.

(34) Thaning, E. M.; Asplund, M. L. M.; Nyberg, T. A.; Inganäs, O. W.; von Holst, H. Stability of poly(3,4-ethylene dioxythiophene) materials intended for implants. *J. Biomed. Mater. Res., Part B* **2010**, *93B* (2), 407−415.

(35) Tayebi; Shahini, A.; Yazdimamaghani, M.; Walker, K.; Eastman, M.; Hatami-Marbini, H.; Smith, B.; Ricci, J. L.; Madihally, S.; Vashaee, D. 3D conductive nanocomposite scaffold for bone tissue engineering. *Int. J. Nanomed.* **2013**, 167.

(36) Cheng, L.; Yang, K.; Chen, Q.; Liu, Z. Organic Stealth Nanoparticles for Highly Effective in Vivo Near-Infrared Photothermal Therapy of Cancer. *ACS Nano* **2012**, *6* (6), 5605−5613.

(37) Sun, K.; Zhang, S.; Li, P.; Xia, Y.; Zhang, X.; Du, D.; Isikgor, F. H.; Ouyang, J. Review on application of PEDOTs and PEDOT: PSS in energy conversion and storage devices. *J. Mater. Sci.: Mater. Electron.* **2015**, *26* (7), 4438−4462.

(38) Yue, K.; Trujillo-de Santiago, G.; Alvarez, M.; Tamayol, A.; Annabi, N.; Khademhosseini, A. Synthesis, properties, and biomedical

DOI: 10.1021/acsbiomaterials.8b00135
ACS Biomater. Sci. Eng. 2018, 4, 1558−1567

applications of gelatin methacryloyl (GelMA) hydrogels. *Biomaterials* **2015**, *73*, 254−271.
(39) Suri, S. S.; Rakotondradany, F.; Myles, A. J.; Fenniri, H.; Singh, B. The role of RGD-tagged helical rosette nanotubes in the induction of inflammation and apoptosis in human lung adenocarcinoma cells through the P38 MAPK pathway. *Biomaterials* **2009**, *30* (17), 3084−3090.
(40) Zhang, L.; Rakotondradany, F.; Myles, A. J.; Fenniri, H.; Webster, T. J. Arginine-glycine-aspartic acid modified rosette nanotube-hydrogel composites for bone tissue engineering. *Biomaterials* **2009**, *30* (7), 1309−1320.
(41) Ramón-Azcón, J.; Ahadian, S.; Obregón, R.; Camci-Unal, G.; Ostrovidov, S.; Hosseini, V.; Kaji, H.; Ino, K.; Shiku, H.; Khademhosseini, A.; Matsue, T. Gelatin methacrylate as a promising hydrogel for 3D microscale organization and proliferation of dielectrophoretically patterned cells. *Lab Chip* **2012**, *12*, 2959.
(42) Nichol, J. W.; Koshy, S. T.; Bae, H.; Hwang, C. M.; Yamanlar, S.; Khademhosseini, A. Cell-laden microengineered gelatin methacrylate hydrogels. *Biomaterials* **2010**, *31* (21), 5536−5544.
(43) Zhou, J.; Anjum, D. H.; Chen, L.; Xu, X.; Ventura, I.; Jiang, L.; Lubineau, G. The temperature-dependent microstructure of PEDOT/PSS films: insights from morphological, mechanical and electrical analyses. *J. Mater. Chem. C* **2014**, *2* (46), 9903−9910.
(44) Patton, A. J.; Green, R. A.; Poole-Warren, L. A. Mediating conducting polymer growth within hydrogels by controlling nucleation. *APL Mater.* **2015**, *3* (1), 014912.
(45) Van Den Bulcke, A. I.; Bogdanov, B.; De Rooze, N.; Schacht, E. H.; Cornelissen, M.; Berghmans, H. Structural and rheological properties of methacrylamide modified gelatin hydrogels. *Biomacromolecules* **2000**, *1*, 31.
(46) Assmann, A.; Vegh, A.; Ghasemi-Rad, M.; Bagherifard, S.; Cheng, G.; Sani, E. S.; Ruiz-Esparza, G. U.; Noshadi, I.; Lassaletta, A. D.; Gangadharan, S. A highly adhesive and naturally derived sealant. *Biomaterials* **2017**, *140*, 115.
(47) Burke, N. J.; Burrows, A. D.; Mahon, M. F.; Teat, S. J. Incorporation of sulfonate dyes into hydrogen-bonded networks. *CrystEngComm* **2004**, *6* (71), 429−436.
(48) Tan, H.; Chu, C. R.; Payne, K. A.; Marra, K. G. Injectable in situ forming biodegradable chitosan hyaluronic acid based hydrogels for cartilage tissue engineering. *Biomaterials* **2009**, *30* (13), 2499−2506.
(49) Lee, K. Y.; Rowley, J. A.; Eiselt, P.; Moy, E. M.; Bouhadir, K. H.; Mooney, D. J. Controlling mechanical and swelling properties of alginate hydrogels independently by cross-linker type and cross-linking density. *Macromolecules* **2000**, *33*, 4291.
(50) Alemu, D.; Wei, H. Y.; Ho, K. C.; Chu, C. W. Highly conductive PEDOT: PSS electrode by simple film treatment with methanol for ITO-free polymer solar cells. *Energy Environ. Sci.* **2012**, *5*, 9662.
(51) Mũnoz, Z.; Shih, H.; Lin, C.-C. Gelatin hydrogels formed by orthogonal thiol−norbornene photochemistry for cell encapsulation. *Biomater. Sci.* **2014**, *2* (8), 1063−1072.
(52) Corradi, R.; Armes, S. P. Chemical synthesis of poly(3,4-ethylenedioxythiophene). *Synth. Met.* **1997**, *84* (1−3), 453−454.
(53) Coletta, C.; Cui, Z.; Dazzi, A.; Guigner, J.-M.; Néron, S.; Marignier, J.-L.; Remita, S. A pulsed electron beam synthesis of PEDOT conducting polymers by using sulfate radicals as oxidizing species. *Radiat. Phys. Chem.* **2016**, *126*, 21−31.
(54) Breukers, R. D.; Gilmore, K. J.; Kita, M.; Wagner, K. K.; Higgins, M. J.; Moulton, S. E.; Clark, G. M.; Officer, D. L.; Kapsa, R. M. I.; Wallace, G. G. Creating conductive structures for cell growth: Growth and alignment of myogenic cell types on polythiophenes. *J. Biomed. Mater. Res., Part A* **2010**, *95A* (1), 256−268.
(55) Horowitz, P. *The art of electronics*, third ed.; Cambridge University Press: New York, 2015; p xxxi.
(56) Zhang, Y.; Ali, S. F.; Dervishi, E.; Xu, Y.; Li, Z.; Casciano, D.; Biris, A. S. Cytotoxicity effects of graphene and single-wall carbon nanotubes in neural phaeochromocytoma-derived PC12 cells. *ACS Nano* **2010**, *4* (6), 3181−3186.
(57) Zhang, X.; Yin, J.; Peng, C.; Hu, W.; Zhu, Z.; Li, W.; Fan, C.; Huang, Q. Distribution and biocompatibility studies of graphene oxide in mice after intravenous administration. *Carbon* **2011**, *49* (3), 986−995.
(58) Li, L.; Ge, J.; Guo, B.; Ma, P. X. In situ forming biodegradable electroactive hydrogels. *Polym. Chem.* **2014**, *5* (8), 2880−2890.
(59) Jun, I.; Jeong, S.; Shin, H. The stimulation of myoblast differentiation by electrically conductive sub-micron fibers. *Biomaterials* **2009**, *30* (11), 2038−2047.
(60) Loffredo, F.; Lee, R. T. Therapeutic Vasculogenesis It Takes Two. *Circ. Res.* **2008**, *103*, 128.
(61) Ai, H.; Lvov, Y. M.; Mills, D. K.; Jennings, M.; Alexander, J. S.; Jones, S. A. Coating and selective deposition of nanofilm on silicone rubber for cell adhesion and growth. *Cell Biochem. Biophys.* **2003**, *38* (2), 103−114.
(62) Davidenko, N.; Schuster, C. F.; Bax, D. V.; Farndale, R. W.; Hamaia, S.; Best, S. M.; Cameron, R. E. Evaluation of cell binding to collagen and gelatin: a study of the effect of 2D and 3D architecture and surface chemistry. *J. Mater. Sci.: Mater. Med.* **2016**, *27* (10), 148.
(63) Taubenberger, A. V.; Woodruff, M. A.; Bai, H.; Muller, D. J.; Hutmacher, D. W. The effect of unlocking RGD-motifs in collagen I on pre-osteoblast adhesion and differentiation. *Biomaterials* **2010**, *31* (10), 2827−2835.
(64) Lampe, K. J.; Antaris, A. L.; Heilshorn, S. C. Design of three-dimensional engineered protein hydrogels for tailored control of neurite growth. *Acta Biomater.* **2013**, *9* (3), 5590−5599.
(65) Straley, K. S.; Heilshorn, S. C. Independent tuning of multiple biomaterial properties using protein engineering. *Soft Matter* **2009**, *5* (1), 114−124.
(66) Monteiro, G. A.; Fernandes, A. V.; Sundararaghavan, H. G.; Shreiber, D. I. Positively and negatively modulating cell adhesion to type I collagen via peptide grafting. *Tissue Eng., Part A* **2011**, *17* (13−14), 1663−1673.
(67) Cukierman, E.; Pankov, R.; Stevens, D. R.; Yamada, K. M. Taking Cell-Matrix Adhesions to the Third Dimension. *Science* **2001**, *294* (5547), 1708−1712.
(68) Kirkpatrick, C. J. Modelling the regenerative niche: a major challenge in biomaterials research. *Regenerative biomaterials* **2015**, *2* (4), 267−272.
(69) Pennesi, G.; Scaglione, S.; Giannoni, P.; Quarto, R. Regulatory influence of scaffolds on cell behavior: how cells decode biomaterials. *Curr. Pharm. Biotechnol.* **2011**, *12* (2), 151−159.
(70) Meng, X.; Stout, D. A.; Sun, L.; Beingessner, R. L.; Fenniri, H.; Webster, T. J. Novel injectable biomimetic hydrogels with carbon nanofibers and self assembled rosette nanotubes for myocardial applications. *J. Biomed. Mater. Res., Part A* **2013**, *101A* (4), 1095−1102.
(71) Chen, Y.; Bilgen, B.; Pareta, R. A.; Myles, A. J.; Fenniri, H.; Ciombor, D. M.; Aaron, R. K.; Webster, T. J. Self-assembled rosette nanotube/hydrogel composites for cartilage tissue engineering. *Tissue Eng., Part C* **2010**, *16* (6), 1233−1243.
(72) Lin Chun, A.; Moralez, J. G.; Webster, T. J.; Fenniri, H. Helical rosette nanotubes: a biomimetic coating for orthopedics? *Biomaterials* **2005**, *26* (35), 7304−7309.
(73) Fine, E.; Zhang, L.; Fenniri, H.; Webster, T. J. Enhanced endothelial cell functions on rosette nanotube-coated titanium vascular stents. *Int. J. Nanomed.* **2009**, *4*, 91−7.
(74) Zhang, L.; Ramsaywack, S.; Fenniri, H.; Webster, T. J. Enhanced osteoblast adhesion on self-assembled nanostructured hydrogel scaffolds. *Tissue Eng., Part A* **2008**, *14* (8), 1353−64.
(75) Zhang, L.; Rodriguez, J.; Raez, J.; Myles, A. J.; Fenniri, H.; Webster, T. J. Biologically inspired rosette nanotubes and nanocrystalline hydroxyapatite hydrogel nanocomposites as improved bone substitutes. *Nanotechnology* **2009**, *20* (17), 175101.
(76) It should be noted that most reported studies on so-called "conductive" hydrogels (including the present one) featured materials with conductivities that are well below the threshold for a true conductor: Le, T.-H.; Kim, Y.; Yoon, H. Electrical and Electrochemical Properties of Conducting Polymers. *Polymers* **2017**, *9* (4), 150. However, all these studies have demonstrated improved electroconductivity via the addition of a conductive material.[11,18,27].

DOI: 10.1021/acsbiomaterials.8b00135
ACS Biomater. Sci. Eng. 2018, 4, 1558−1567